# Coupled Plasma-Electrode Simulation of the Free-Burning Arc using a Chemical and Thermal Non-Equilibrium Model

P. Liang[1], V. D. Boutrouche[1], and J. P. Trelles[1]

[1] *Department of Mechanical Engineering, University of Massachusetts Lowell, 1 University Ave, Lowell, MA 01854, USA*

**Abstract:** Energy transfer phenomena between plasma and its operating electrodes play a key role in typical arc discharge applications, such as arc welding or plasma cutting. Reliable numerical predictions are highly desired to optimize the performance or extend the lifetime of the discharge system. A coupled plasma-electrodes model is presented and applied to the three-dimensional simulation of the free-burning arc. The model couples a chemical and thermal non-equilibrium plasma flow model with models for the metal electrode domains and of the non-neutral space-charge layer, eliminating the need of ad-hoc or inconsistent boundary conditions often encoutered in arc discharge models.

**Keywords:** plasma-electrode coupling, chemical and thermal non-equilibrium

## 1. Introduction

Typical direct current (DC) arc systems, such as arc welding or plasma cutting, involve an anode, cathode, and the working gas. The anode is typically water-cooled to prevent unwanted evaporated anode material from contaminating the working gas. Despite all these configurations, under high discharge current intensities, the elements including anode and cathode still get easily eroded or destructed, which could undermine the system performance and its lifetime as well. Thus, the control of arc discharge systems could not be realized without adequate knowledge of its main characteristics temperature development especially in the plasma body. Thermal and chemical non-equilibrium characteristics are often encountered in arc plasma system. The former is often encountered at the arc fringes and near-electrode regions, where the heavy-species temperature drops drastically whereas the electron temperature remains significantly higher. This has been both theoretically and experimentally reported by many authors [1-3]. The latter is mainly quantified by the imbalance between collisional ionisation and three-body recombination among heavy-species and electrons, which is due to the fact that chemical reactions often fail to follow the fast macroscopic translation of charged particles in plasma [4]. Therefore, numerical simulations that account for both types of non-equilibirum are highly sought after.

Coupled plasma-electrode models have many advantages over models that only account for the plasma region. On one hand, the plasma-only model only takes into account the transport process within the plasma itself and ignores any effect coming from/to either cathode or anode, which could limit the predictive capabilities of the model. On the other hand, numerical simulation using a plasma-only model necessarily rely on ad-hoc aproximations to describe boundary conditions over the electrodes, which are often based on limited experimental results. In a coupled plasma-electrodes model, these boundary conditions are not necessary since the plasma-electrode interface is within the computational domain, and therefore it is resolved by the simulation. The development of a coupled plasma-electrodes model faces the additional challenge to describe the space-charge layer (typically referred to the electrode sheath), which cannot be described by a plasma flow model that relies on the assumption of quasi-neutrality. Therefore, a couple plasma-electrodes model needs to count with appropriate so-called sheath models to describe the plasma-electrode interfaces.

This paper describes three-dimensional simulation of the free-burning arc using a mathematical model that couples a chemical and thermal non-equilibrium plasma flow model with models for the metal electrode domains and of the non-neutral space-charge layer, eliminating the need of ad-hoc or inconsistent boundary conditions often encoutered in arc discharge models. The sheath layer model combines the properties of both collisionless sheath and collisional bulk plasma properties to determine an effective electrical conductivity. A more detailed description of the model is found in [5].

## 2. Mathematical model

The model relies on the assumption that no erosion or evaporation of electrodes (copper anode and thoriated tungsten cathode), as well as dielectric steel nozzle, occurs. The model also neglects the effect of gravity in the momentum equation, and viscous dissipation in the energy equation for the heav-species.

The chemical non-equilibrium model of argon considers up to triple-ionization, i.e. $Ar^{3+}$ ions. The set of transport equations comprising the model is shown in Table 1. The model is implemented as a base solver in the open-source Computational Fluid Dynamics (CFD) software OpenFOAM. The PISO algorithm [6] is applied to perform the pressure correction and velocity coupling. As high temperature plasmas are largely characterised by high macroscopic flow speeds, the discretisation schemes of convection terms are all second-order accurate and fulfil the Total Variation Diminishing (TVD) criterion by using Sweby's Limiter [7], which helps ensure numerical stability.

Table 1: Transport equations for chemical and thermal non-equilibrium plasma as well as metal electrodes. For each equation: Transient + Advective – Diffusive − Reactive = 0.

| Equation | Transient | Advective | Diffusive | Reactive |
|---|---|---|---|---|
| Conservation of heavy species | $\partial_t n_i$ | $\boldsymbol{u} \cdot \nabla n_i + n_i \nabla \cdot \boldsymbol{u}$ | $-\nabla \cdot \boldsymbol{j}_{\boldsymbol{D},\boldsymbol{i}}$ | $\omega_i \quad (i = 0\sim3)$ |
| Conservation of linear momentum | $\rho \partial_t \boldsymbol{u}$ | $\rho \boldsymbol{u} \cdot \nabla \boldsymbol{u} + \nabla p$ | $\nabla \cdot \boldsymbol{\tau}$ | $\boldsymbol{J}_q \times \boldsymbol{B}$ |
| Thermal energy (heavy-species) | $\rho \partial_t h_h$ | $\rho \boldsymbol{u} \cdot \nabla h_h$ | $\nabla \cdot (\kappa_h \nabla T_h)$ | $D_t p_h + K_{eh}(T_e - T_h) + p_e \nabla \cdot \boldsymbol{u} + \boldsymbol{u} \cdot (\boldsymbol{J}_q \times \boldsymbol{B})$ |
| Thermal energy (electrons) | $\rho \partial_t h_e$ | $\rho \boldsymbol{u} \cdot \nabla h_e$ | $\nabla \cdot (\kappa_e \nabla T_e)$ | $D_t p_e - K_{eh}(T_e - T_h) - 4\pi\varepsilon_r + \boldsymbol{J}_q \cdot (\boldsymbol{E} + \boldsymbol{u} \times \boldsymbol{B}) + \frac{5k_B}{2e} \boldsymbol{J}_q \cdot \nabla T_e - \nabla \cdot (\frac{5}{2} k_B T_e \boldsymbol{j}_{\boldsymbol{D},e}) - \sum_{\boldsymbol{i}=\boldsymbol{1}}^{3} \omega_i E_i$ |
| Thermal energy (electrodes) | $\rho \partial_t h_s$ | 0 | $\nabla \cdot (\kappa_s \nabla T_s)$ | $\boldsymbol{J}_s^2 / \sigma_s$ |
| Charge conservation | 0 | 0 | $-\nabla \cdot \boldsymbol{J}_q$ | 0 |
| Magnetic induction | $\partial_t \boldsymbol{A}$ | $\nabla \phi_p - \boldsymbol{u} \times (\nabla \times \boldsymbol{A})$ | $(\mu_0 \sigma)^{-1} \nabla^2 \boldsymbol{A}$ | $\boldsymbol{0}$ |

In the model, the species conservation equations for argon species, characterizing chemical non-equilibrium, account for ambipolar diffusion and inelastic collisions. The model of multi-species diffusion is taken from [8] to ensure that total diffusion fluxes satisfy overall mass conservation, i.e. $\sum_{i=0}^{3} \boldsymbol{j}_{\boldsymbol{D},\boldsymbol{i}} = 0$. In addition, the reactive terms that describe ionization reactions also add up to zero, ensuring that total mass conservation is fulfilled.

For the coupled simulations considered in this work, energy transport within the electrodes also needs to be solved. The electrode energy conservation equation describes the evolution of the temperature $T_s$, which is connected to the heavy-species temperature $T_h$ at the plasma-electrode interface by an energy conservation relation. The two temperatures of the plasma ($T_h$ and $T_e$) are coupled by the energy exchange term $K_{eh}(T_e - T_h)$, where the coefficient $K_{eh}$ is derived from the elastic collision frequencies between electrons and heavy-species.

All the transport properties of argon plasma needed in the simulation such as electrical conductivity $\sigma$ and thermal conductivities of heavy-species $\kappa_h$ and electrons $\kappa_e$, are calculated according to Chapman-Enskog method [9].

An important and demanding step in building a coupled plasma-electrode interaction model is the incorporation of sheath layer model. The one-fluid two-temperature plasma flow model cannot describe this layer, due to its characteristic non-neutrality. The sheath's actual dimension is usually only of the order of $10^{-8}$ m, which could hardly be represented by CFD meshes due to associate large computational cost. Hence, the boundary cells, which are the first row of cells on the interface, are chosen to represent the sheath. An effective electrical conductivity for the sheath is applied over the boundary cells, which has the following form:

$$\sigma_{eff} = \frac{1}{\frac{1}{\sigma_c}(1 - I_g) + \frac{1}{\sigma} I_g}, \tag{1}$$

where $\sigma_c$ is the electrical conductivity derived from Child's Law of space-charge limited current [10], and $\sigma$ is the electrical conductivity calculated for the bulk plasma. These two values are then harmonically averaged by the local ionization degree $I_g$. When $I_g$ approaches 0, $\sigma_{eff}$ will reflect the value of $\sigma_c$, which corresponds to a collisonless sheath; otherwise, boundary cells will have the property of the collision-dominated bulk plasma, since their value approach $\sigma$. Through this model, the sheath layer is successfully hided into the boundary cells and mixed with bulk plasma properties. The conservation of electric current could then be obtained by applying Ohm's law on both sides of the plasma-electrode interface:

$$\sigma_{eff}\frac{\varphi_{cp}-\varphi_p}{\Delta x_p} = \sigma_s\frac{\varphi_p-\varphi_{cs}}{\Delta x_s} \text{ (cathode sheath),} \tag{2}$$

where the subscript *cp*, *p* and *cs* denote cell center of the plasma, patch, and cell center of the solid electrode, respectively. As the anode sheath is not considered in this work, σ instead of $\sigma_{eff}$ is applied on the plasma side, i.e.:

$$\sigma\frac{\varphi_{cp}-\varphi_p}{\Delta x_p} = \sigma_s\frac{\varphi_p-\varphi_{cs}}{\Delta x_s} \text{ (other interfaces).} \tag{3}$$

Using such relation, the continuity of electric potential through the interface is secured.

## 3. Results

The coupled plasma-electrode simulations correspond to an operating current of 200 A, which is imposed at the cold end of the cathode, and 10 slpm gas flow rate at nozzle inlet. The temperature fields of are initiated at 500 K for $T_h$ and 5000 for $T_e$ to make electrical conductivity high enough to establish a discharge. The anode bottom is assumed to be water-cooled and a fixed value of 500 K is defined over its bottom surface. Fig. 1 shows the results of the two temperature fields. The distribution of $T_e$ is more diffusive than that of $T_h$. This is related to the much smaller mass of electrons in comparison with that of the heavy-species ($m_e/m_h \sim 10^{-5}$), which makes electrons more effective at acquiring energy from the imposed DC field. In the arc core, due to the high $T_e$ value, the local electron number density $n_e$, as well collision frequencies, are high enough to keep energy transfer from electron to heavy-species active. Therefore, $T_h$ in this region has almost the same value as $T_e$. Fig. 2 shows the ratio of $T_e$ to $T_h$, which is denoted as the thermal nonequilibrium parameter θ. The highest degree of thermal non-equilibrium appears at the fringes of the arc, which is due to the limited energy exchange between electrons and heavy-species, as described by the term $K_{eh}(T_e - T_h)$. It can also be noted that near the cathode and anode surfaces the value of θ rises drastically, as the value of $T_h$ needs to be in balance with the surface temperature of metal electrodes $T_s$, which is usually much lower than the ambient electron temperature.

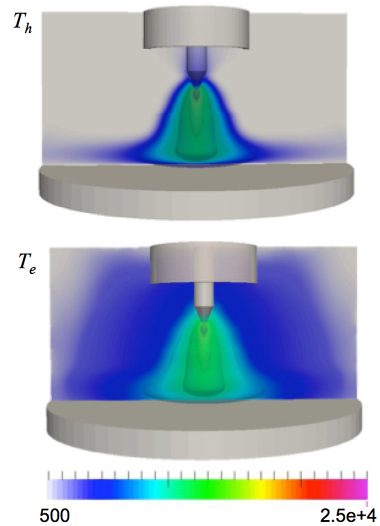


Fig. 1. Numerical results of the chemical and thermal non-equilibrium argon plasma model (bottom: electron temperature; top: heavy species temperature).

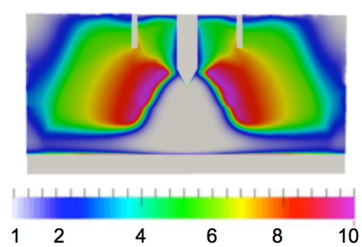


Fig. 2. Degree of thermal non-equilibrium $\theta$ ($T_e/T_h$).

Figure 3 shows the coupled electromagnetic fields. Due to the application of Eq. 2 and Eq. 3, these fields evolve continuously throughout the whole domain. The results show a large gradient at the boundary cells near the cathode. The use of $\sigma_{eff}$ along these cells makes them act as a "mixture layer" to represent a transition from space-charge sheath to collision-dominated bulk plasma.

The obtained number densities from the solution of the species conservation equations are compared with those from Saha's ionization equilibrium in Fig. 4. The results in this figure show that the equilibrium and non-equilibrium results of both electron and singly charged ions are comparable in both, the arc core and outer regions of computation domain. In contrast, they significantly differ from each other at the arc fringes. The maximum ratio of non-equilibrium to equilibrium number density is as high as $10^6$, which indicates that ambipolar diffusion plays a dominant role over ionization non-equilibrium in these regions. Comparable trends and relations between equilibrium and nonequilibrium number densities are reported in the numerical results of Baeva et al. [11], which considered only a single level of ionization. The difference between the results of electron and singly charged argon could be observed in the near-anode region, where ratio of $n_e/n_e|_{eq}$ is larger than $n_{Ar^+}/n_{Ar^+}|_{eq}$, which appears to be a result of the mass diffusion of $Ar^{2+}$ and $Ar^{3+}$. In the places where the ratio is lower than 1, three-body recombination dominates over all the other effects.

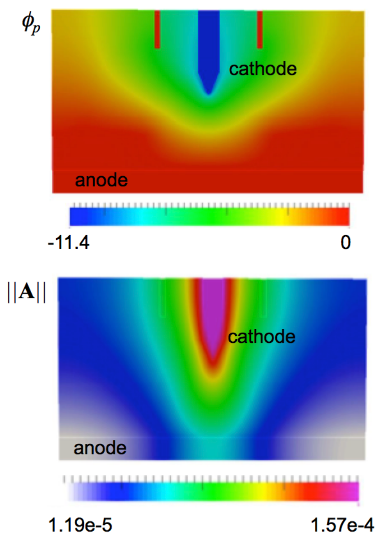


Fig. 3. Electromagnetic fields across the coupled plasma-electrodes domain (top: electric potential; bottom: magnitude of magnetic vector potential).

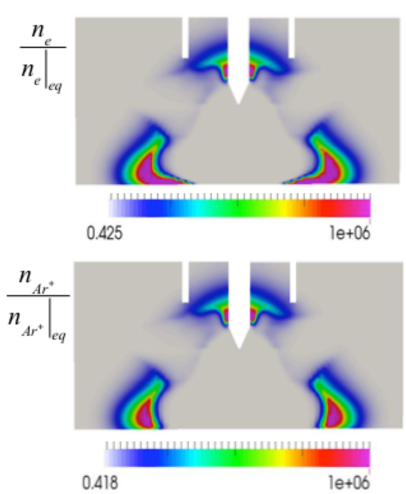


Fig. 4. Comparison of number densities in argon plasma obtained by chemical equilibrium ($|_{eq}$) and non-equilibrium methods (top: electrons; right: singly-charged argon ions).

## 4. Conclusions

A coupled plasma-electrodes model has been developed and applied to the thermal and chemical nonequilibrium simulation of the free-burning arc. A sheath layer model is incorporated into the model to describe the plasma-cathode interface by using an effective sheath conductivity through the interface cells. A large electric potential drop is captured by this method, which at the same time secures continuous transition of electromagnetic fields through the whole system. The results of both chemical equilibrium and non-equilibrium number densities are discussed, leading to the conclusion that ambipolar diffusion plays a dominant role at the arc fringes, which makes the assumption of a chemical equilibrium composition invalid at those regions.

**Acknowledgements**

The authors acknowledge financial support from the U.S. Department of Energy through award DE-SC0018230.

**References**

[1] J.F. Bott. Spectroscopic measurement of temperatures in an argon plasma arc. Phys. Fluids. 9:1540-1547. (1966).

[2] L.E. Cram, L. Poladian and G. Roumellotis. Departures from equilibrium in a free-burning argon arc. J.Phys.D: Apply.Phys. 21:418-425,(1988).

[3] C.H. Chang and J.D. Ramshaw. Numerical Simulation of nonequilibrium effects in an argon plasma jet. Phys. Plasmas 1(11):3698-3708, (1994).

[4] C.H.Chang and E. Pfender. Nonequilibrium Modeling of Low-Pressure Argon Plasma Jets; Part I: Laminar Flow. Plasma Chem. And Plasma Proc. 10:473-491,(1990).

[5] P. Liang. 2D-Self-consistent modeling of arc-electrode interaction in GTAW using a finite volume method. J. Phys. D: Appl. Phys. 52:035203,(2019).

[6] R.I.Issa. Solution of the Implicitly Discretised Fluid Flow Equations by Operator-Splitting. J. Comput. Phys. 62:40-65, (1986).

[7] P.K.Sweby. High Resolution Schemes Using Flux Limiters for Hyperbolic Conservation Laws. SIAM J. Numer. Anal. 21:995-1011,(1984).

[8] M.Fertig, A.Dohr and H.H. Frühauf. Transport Coefficients for High Temperature Nonequilibrium Air Flows. 7th AIAA/ASME Joint Thermophysics and Heat Transfer Conference, Albuquerque, NM, (1998).

[9] S. Chapman and T.G. Cowling. The mathematical theory of non-uniform gases. London:Cambridge University Press,(1939).

[10] C.D.Child. Discharge from hot CaO. Phys. Rev.I, 32:492-51,(1911).

[11] M. Baeva. A Survey of Chemical Nonequilibrium in Argon Arc Plasma. Plasma Chem. Plasma Proc. 37:513-530, (2017).